



Electrostatic analysis of TEM1 -lactamase: effect of substrate binding, steep potential gradients and consequences of site-directed mutations

Peter Swarén, Laurent Maveyraud, Valérie Guillet, Jean-Michel Masson,
Lionel Mourey, Jean Pierre Samama

► To cite this version:

Peter Swarén, Laurent Maveyraud, Valérie Guillet, Jean-Michel Masson, Lionel Mourey, et al.. Electrostatic analysis of TEM1 -lactamase: effect of substrate binding, steep potential gradients and consequences of site-directed mutations. *Structure*, 1995, 3 (6), pp.603-613. 10.1016/s0969-2126(01)00194-0 . hal-03004753

HAL Id: hal-03004753

<https://cnrs.hal.science/hal-03004753>

Submitted on 20 Nov 2020

HAL is a multi-disciplinary open access archive for the deposit and dissemination of scientific research documents, whether they are published or not. The documents may come from teaching and research institutions in France or abroad, or from public or private research centers.

L'archive ouverte pluridisciplinaire **HAL**, est destinée au dépôt et à la diffusion de documents scientifiques de niveau recherche, publiés ou non, émanant des établissements d'enseignement et de recherche français ou étrangers, des laboratoires publics ou privés.

Electrostatic analysis of TEM1 β -lactamase: effect of substrate binding, steep potential gradients and consequences of site-directed mutations

Peter Swarén^{1,2}, Laurent Maveyraud¹, Valérie Guillet¹,
Jean-Michel Masson³, Lionel Mourey¹ and Jean-Pierre Samama^{1*}

¹Groupe de Cristallographie Biologique, Laboratoire de Pharmacologie et de Toxicologie Fondamentales du CNRS, 205 route de Narbonne, F-31077 Toulouse CEDEX, France, ²Department of Physical Chemistry, Chalmers University of Technology, S-412 96 Gothenburg, Sweden and ³Groupe d'Ingénierie des Protéines, Laboratoire de Pharmacologie et de Toxicologie Fondamentales du CNRS, 205 route de Narbonne, F-31077 Toulouse CEDEX, France

Background: *Escherichia coli* TEM1 is a penicillinase and belongs to class A β -lactamases. Its naturally occurring mutants are responsible for bacterial resistance to β -lactamin-based antibiotics. X-ray structure determinations show that all class A β -lactamases are similar, but, despite the numerous kinetic investigations, the reaction mechanism of these enzymes is still debated. We address the questions of what the molecular contexts during the acylation and deacylation steps are and how they contribute to the efficiency of these penicillinases.

Results: Electrostatic analysis of the 1.8 Å resolution refined X-ray structure of the wild-type enzyme, and of its modelled Michaelis and acyl-enzyme complexes, showed that substrate binding induces an upward shift in the pK_a of the unprotonated Lys73 by 6.4 pH units. The amine group of Lys73 can then abstract the Ser70 hydroxyl group proton and promote acylation. In the acyl-enzyme complex, the deacylating water is situated between the carboxylate

group of Glu166, within the enzyme, and the ester-carbonyl carbon of the acyl-enzyme complex, in an electrostatic potential gradient amounting to 30 kTe⁻¹ Å⁻¹. Other residues, not directly involved in catalysis, also contribute to the formation of this gradient. The deacylation rate is related to the magnitude of the gradient. The kinetic behaviour of site-directed mutants that affect the protonation state of residue 73 cannot be explained on the basis of the wild-type enzyme mechanism.

Conclusions: In the wild-type enzyme, the very high rates of acylation and deacylation of class A β -lactamases arise from an optimal chemical setup in which the acylation reaction seems triggered by substrate binding that changes the general base property of Lys73. In site-directed mutants where Lys73 is protonated, acylation may proceed through activation of a water molecule by Glu166, and Lys73 contributes as a proton shuffle partner in this pathway.

Structure 15 June 1995, 3:603–613

Key words: antibiotics, β -lactamase, electrostatics, hydrolysis, substrate-triggered mechanism

Introduction

Extensive use of antibiotics in the community and in hospitals has caused bacteria to become resistant to these agents. The resistance is mainly mediated by the β -lactamase enzymes and is spread by plasmid exchange. Selection pressure favours the emergence of mutant enzymes that exhibit extended substrate specificities. Among all mutant enzymes in resistant bacteria, the majority have evolved from *Escherichia coli* TEM1 β -lactamase.

Considerable work has been aimed at describing the structure–function relationships of the β -lactamases. However, rationalization of experimental data is difficult to achieve, because, except for the partition between classes A, B, and C proposed by Ambler *et al.* [1], based on sequence alignment, the borderline defined by some of the characteristics of the enzymes, such as evolutionary propensity, response to clavulanic acid, or genetic origin, is not always straightforward. This explains why other classification schemes have been proposed [2].

Class A β -lactamases are penicillinases. They are all very efficient enzymes with nearly diffusion-controlled kinetics. After formation of the enzyme=substrate Michaelis complex (k_1, k_{-1}), a tetrahedral intermediate leads to the acyl-enzyme complex (k_2). The reaction product is released after hydrolysis of this complex by a water molecule (k_3) through the formation of another tetrahedral intermediate. Acylation and deacylation steps have both similar and very high rate constants (for example, $k_2=2800\text{ s}^{-1}$, $k_3=1500\text{ s}^{-1}$ for *E. coli* TEM1, with benzylpenicillin as substrate) [3]. Several X-ray structures of class A β -lactamases have been solved. Enzymes from the Gram-positive bacteria *Streptomyces albus* G [4], *Staphylococcus aureus* PC1 [5] and *Bacillus licheniformis* 749/C [6], and the TEM1 enzyme from the Gram-negative *E. coli* [7–9] all have similar structures. Jelsch *et al.* [9] described the main differences between TEM1 and the Gram-positive enzymes at 1.8 Å resolution. Among these differences are the relative orientations of the two domains comprising the enzyme, which creates a narrowed substrate cavity

*Corresponding author.

in TEM1. All class A β -lactamases contain the invariant active-site residues Ser70, Lys73, Glu166, and Lys234 (residue numbering according to Ambler *et al.* [1]), to which have been attributed various plausible functions in the mechanism of the enzymes [10,11]. A reaction scheme has been proposed for these β -lactamases from the X-ray structure determination of the acyl-enzyme complex trapped in the deacylation-defective Glu166 \rightarrow Asn TEM1 mutant protein [8]. In this mechanism, as hypothesized by Oefner *et al.* [12], the unprotonated Lys73 acts as a general base that assists the nucleophilic attack of Ser70 O γ on the substrate. However, a depressed pK_a value of Lys73 in the free enzyme does not explain why acylation occurs and why this reaction is so fast. The high rate constants would suggest that, in the wild-type (WT) enzyme, the chemical events occurring in the catalytic steps have minimal or lowered energy barriers, which are likely to be provided by an optimal chemical environment. As enzyme catalysis involves acid-base chemistry and charge transfers, it seemed appropriate to address the mechanism of β -lactamase action by electrostatic analysis of the enzyme's refined structure.

Results and discussion

Control of parameters

From the network of interactions within the active site of TEM1, we used the electrostatic interaction (Table 1) between the buried and proximate Asp214 and Asp233 residues as a reference for our pK_a calculations. The 2.8 Å distance between Asp214 O δ 2 and Asp233 O δ 1 implies that one of these aspartates will be protonated at pH 7.8, the pH at which crystallization and structure determination of TEM1 were carried out [9]. Arguments that point out Asp214 as being protonated resulted from sequence and structural comparisons [9]. Briefly, Asp233 is invariant within the class A β -lactamases and forms a salt bridge with Arg222, while residue 214 is generally an asparagine. The calculation gave a pK_a of 7.6 for Asp214, consistent with the structural and sequence analysis. The pK_a shift of +3.7 pH units (Table 2) from free aspartyl to that in the WT enzyme is in the range expected for a residue buried within the protein structure [13]. In this test calculation, Lys73 was assumed to be protonated. If Lys73 was in the unprotonated state, the tendency for Asp214 to be protonated would be slightly stronger due to the removal of one positive charge at 11.3 Å from Asp214 O δ 2 (Fig. 1). The shift we obtained in the pK_a of Asp214 therefore represents a minimum value. In all subsequent calculations, we assumed Asp214 to be protonated. A second test calculation was performed on Lys146. As the surface residue with the most solvent-accessible ionizable group, its pK_a should remain rather unshifted relative to the free amino acid, but at pH 7.8 the overall negative charge of the protein (pI=5.4 [14]) will attract protons and one could expect a slightly positive shift. Indeed, the computation gave a pK_a shift of +0.4 for Lys146 (Table 2). The latter computation was made with Lys73 unprotonated and, therefore, represents the upper limit of the shift.

Table 1. Electrostatic interaction energies (not including desolvation effects) in the native WT enzyme and its Michaelis complex.

Interaction	WT enzyme* (kT)	Michaelis complex* (kT)
Ser70–Lys73 [†]	–45.75	–51.62
Ser70–Glu166	18.56	23.41
Ser70–H2 α -helix [‡]	–6.86	–8.31
Lys73–Glu166 [†]	–27.53	–31.75
Lys73–Lys234 [†]	14.83	19.57
Asp214–Asp233	28.09	28.81
Ser70–COO [–] (Pen G)	–	42.25
Lys73–COO [–] (Pen G) [†]	–	–23.06
Lys234–COO [–] (Pen G)	–	–66.04
Arg244–COO [–] (Pen G)	–	–9.20

*The interaction energies between complete side chains were computed with each side chain in its ionized state. Interior and exterior dielectrics were set to 3 and 80, respectively.

[†]Protonated Lys73 is relevant in the Lys234 \rightarrow Thr enzyme.

[‡]The H2 α -helix was assigned a charge distribution (overall neutral) only to its backbone atoms. The requirement of lysine or arginine at position 73 for measurable activity [43] indicates that the interaction between Ser70 and the H2 α -helix has a minor role in the activation of Ser70.

Table 2. Calculated differences in Born solvation and background charge interaction energies with corresponding pK_a shifts.

Protein	Residue	$\Delta\Delta G_{\text{Born}}^*$ (kT)	$\Delta\Delta G_{\text{back}}^*$ (kT)	ΔpK_a^{\dagger}
WT	Ser70	–26.91	32.24	–2.31
WT Michaelis complex [‡]	Ser70	–33.05	–19.93	+23.01
WT Michaelis complex (transferred O8 charge) [‡]	Ser70	–29.58	1.65	+12.13
Lys234 \rightarrow Thr	Ser70	–25.19	37.36	–5.29
Lys234 \rightarrow Thr Michaelis complex [‡]	Ser70	–30.82	–5.81	+15.91
WT	Lys73	44.43	–38.62	–2.52
WT Michaelis complex	Lys73	47.05	–56.08	+3.92
Lys234 \rightarrow Thr	Lys73	43.16	–48.80	+2.45
Lys234 \rightarrow Thr Michaelis complex	Lys73	45.37	–68.09	+9.87
WT	Lys146	1.05	–1.99	+0.41
WT	Asp214	–16.06	7.49	+3.72
Lys234 \rightarrow Thr with penicillanyl alcohol	Ser70	–30.82	29.88	+0.41

*The differences are taken as the energy for the protonated state minus that for the unprotonated state. [†] ΔpK_a is the shift of the side chain pK_a in the protein compared with the free amino acid. [‡]The Ser70 pK_a in the Michaelis complexes is poorly estimated by the computations (see text). For an explanation of the terminology, see the Materials and methods section.

Electrostatic potential maps

The enzyme is surrounded by a cloud of negative electrostatic potential which is disrupted in places by several small positive lobes, generated by solvent-accessible lysine and arginine residues at the protein–solvent interface. This mainly negative envelope could be expected since the calculations were performed with a charge set corresponding to a pH value about two units above the isoelectric point of 5.4. At pH 7.8, the protein carries a net negative charge and presents an evenly distributed negative potential on its surface. On a +0.5 kTe^{–1} contour level, solvent

shielding prevents the potential from extending further into solution except for a large funnel-shaped positive lobe, which forms a continuous path from bulk solvent towards the substrate-binding site (Fig. 2). Since Lys215 is the only basic residue found in this region, this feature may indicate a pathway dedicated to attracting the substrate into its binding site with maximal efficiency.

One important feature of the electrostatic potential is its bipolar distribution in the area of the substrate-binding site (Fig. 3). Most of the domain organized about the β -strands is immersed into a $+20 \text{ kTe}^{-1}$ continuous positive potential: residues 234–238 from strand S3, residues 241–245 from strand S4, the first half of the C-terminal helix (residues 270–280), the H2 3_{10} -helix (residues

Fig. 1. Stereoview of the environment around Asp214. The interaction between Asp214 and Asp233 and the salt bridge between Arg222 and Asp233 are both shown with dashed lines as well as the distance between the active site Lys73 and Asp214. Crystallographic waters are indicated by dots. (Figures 1 and 4 generated using MOLSCRIPT [44].)

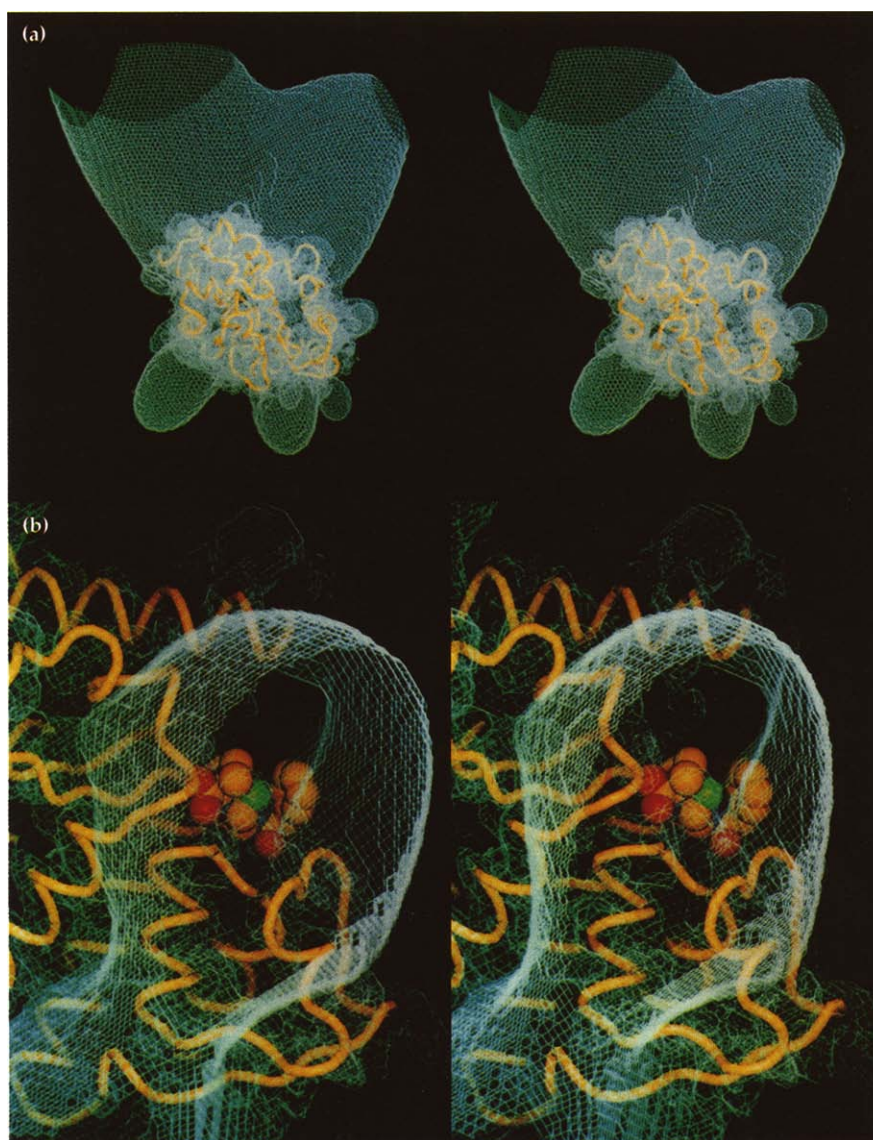
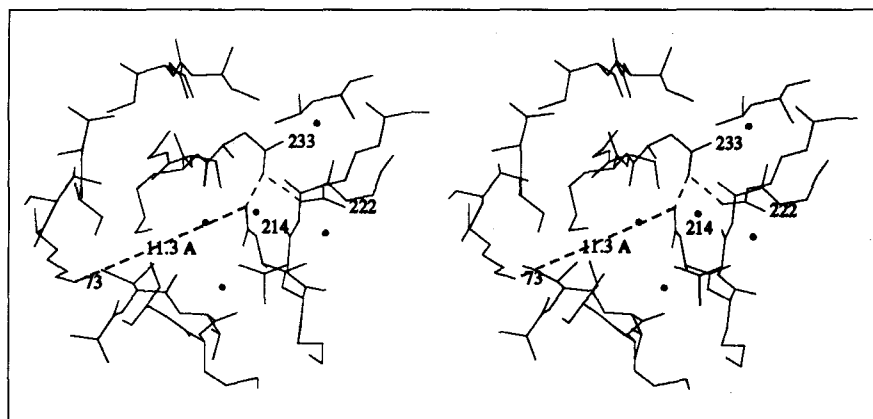


Fig. 2. (a) Map at $+0.5 \text{ kTe}^{-1}$ of the electrostatic potential of TEM1 β -lactamase, obtained after the second focusing step (see the Materials and methods section). (b) Enlarged perpendicular view of (a) showing the continuous path towards the substrate-binding site. Bound Pen G is shown as a space-filling model. (Figures 2, 3, 6, and 7 generated using O [30].)

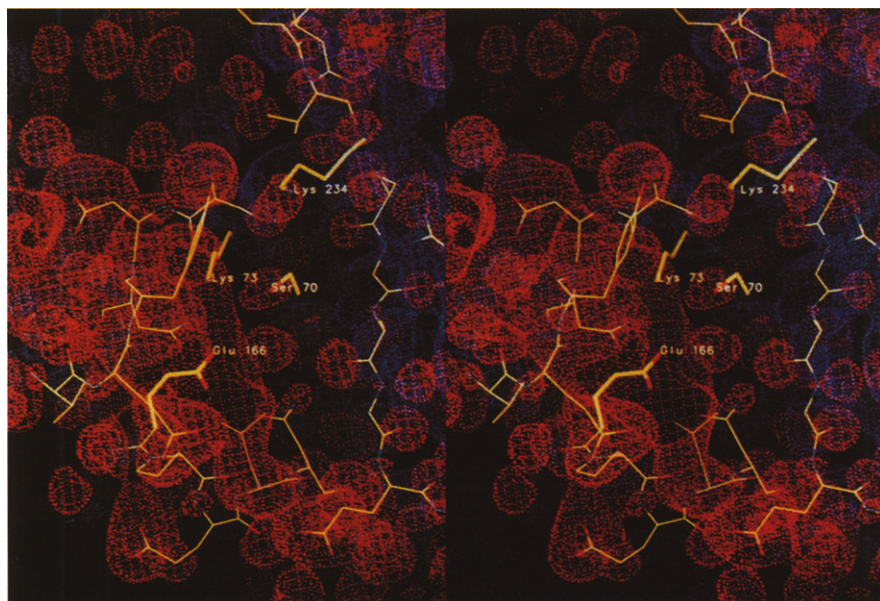


Fig. 3. Bipolar distribution of the electrostatic potential in the area of the substrate-binding site. The $+20 \text{ kTe}^{-1}$ contour is blue and the -20 kTe^{-1} contour is red. The invariant residues of the active site are labelled.

69–71), and the hinge region 213–218. This positive potential arises mainly from residues Lys215, Arg222, Lys234, Arg244, and Arg275. At the other side of the substrate cavity, a -20 kTe^{-1} continuous negative potential surrounds the side-chains of residues 104, 105, 109, 110, 131–133, 136, 163, 166, 168, 170, 179, and 240 and the main-chain oxygen atoms of residues 103–106, 125, 129–132, 161, 167, 169, 170, and 179. As a consequence, the thiazolidine and β -lactam rings of the substrate, whose *re* face is oriented towards the negative potential when bound to the enzyme, are located in a narrow and low potential area (-5 to $+5 \text{ kTe}^{-1}$) between the positive and negative potential domains. In agreement with the kinetic data [15,16], and as already discussed from the X-ray structure [9], before the β -lactam ring opening, the carboxylate group at C3 of the thiazolidine ring is oriented in the Michaelis complex towards the positive potential area and is 2.7 \AA and 3.9 \AA from Lys234 and Arg244, respectively (Fig. 4a). In the acyl-enzyme complex, after the -35° rotation about the N4–C5–C6–C7 torsion angle following the hydrolysis of the β -lactam ring, the carboxylate was observed at 3.5 \AA and 2.7 \AA from Lys234 and Arg244, respectively [8] (Fig. 4b).

Active-site residues

Kinetic studies demonstrated that lysines 73 and 234 are essential amino acids in the mechanism of the enzyme [17–20], and many hypotheses about their functions have been put forward. The pH dependence of k_{cat} in the TEM1 enzyme suggests that a group at about pK_a 10 must be protonated for maximal activity. Analysis of the X-ray structure shows that the only candidate in the substrate-binding area is Lys234.

Since all steps in catalysis involve proton transfers and charged groups, their respective locations and electrostatic environments were examined. We calculated the pK_a of Lys73 in the free WT enzyme to be 8.0, which suggests that two enzyme populations (unprotonated and

protonated Lys73) are able to form Michaelis complexes at pH 7.8. The 5.6 \AA distance between Lys73 and Lys234 N ζ atoms and the inaccessibility to bulk solvent contribute to this pK_a shift from 10.5, for the free amino acid (Table 2). The shift does not, however, explain why acylation occurs, as it describes the physico-chemical state of the enzyme in equilibrium.

We therefore computed the pK_a shift that occurs in the Michaelis complex (Fig. 4a) and found that, upon binding, the benzylpenicillin (Pen G) substrate increases the pK_a of Lys73 to 14.4 prior to any proton transfer. This shift essentially occurs because one negative charge, located 4.5 \AA from Lys73 N ζ , is introduced by the carboxylate at C3 of the thiazolidine ring (Table 2). About 15 kT (9 kcal mol^{-1}) are provided by protonation of a group at pK_a 14.4, compared with protonation of the same group at pK_a 8.0, and we propose that protonation of Lys73 at the Michaelis complex stage may contribute by lowering the energy barrier for Ser70 O γ deprotonation and thereby favour the concerted nucleophilic attack on the substrate C7 atom by the Ser70 O γ free electron pair (Fig. 5a). This proposal leads to a single-proton-transfer mechanism for acylation, which has been favoured by free energy considerations [21] and semi-empirical molecular orbital calculations [22] on serine proteases. The bell-shaped k_{cat}/K_M versus pH profile for the WT enzyme, with phenoxymethylpenicillin as a substrate, shows two ionizations, at $\text{pK}_1=5.0$ and $\text{pK}_2=8.6$, between which maximum activity is attained [18]. pK_2 is in good agreement with the calculated pK_a of Lys73 ($\text{pK}_a=8.0$), while pK_1 is close to the expected pK_a of the Glu166 side chain.

A second Michaelis complex population is formed with protonated Lys73. However, in this kinetic pathway all elementary rate constants are 10 to 100-fold lower [3,17] and negligible compared with those provided by the unprotonated Lys73 population in the WT enzyme [3].

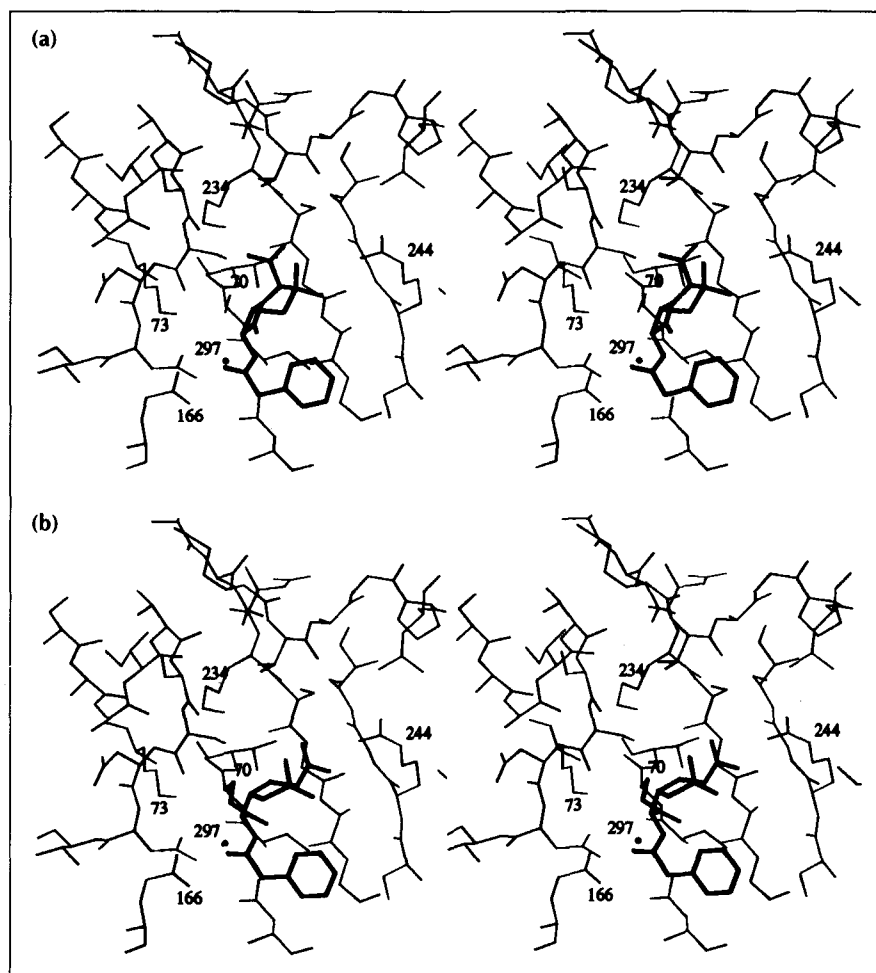


Fig. 4. Stereoviews of the Pen G substrate (thick lines) and the catalytic site of TEM1 (thin lines) (a) in the Michaelis complex and (b) in the acyl-enzyme complex. The deacylating water molecule, Wat297, is represented by a dot. In (b), the ester bond and the side-chain of Ser70 have also been drawn with thick lines.

This pathway becomes the only possible one with site-directed mutant enzymes where residue 73 is protonated, and will be discussed later.

Ser70 O γ is located only 3.5 Å from the substrate carboxylate, which, in the computation of pK_a shifts within the Michaelis complex, resulted in the Ser70 pK_a being raised from 13.7 in the free enzyme to 39.0 after substrate binding and prior to proton transfer to Lys73. This suggests that the Ser70 O γ should be strongly deactivated in the Michaelis complex and a poor nucleophile in the acylation reaction, which is in contrast to the observed fast formation of the acyl-enzyme complex. The electrostatic approach in evaluating the pK_a of Ser70 in the Michaelis complex may be inappropriate for several reasons. First, Ser70 O γ is at bond formation distance from the substrate C7 atom. Second, local variations in dielectric properties, which may be important at the reaction centre, are ignored in the continuum approach. Third, a force field charge distribution that implies an identical description of all residues is used, which might also be incorrect at the reaction centre. And, fourth, the charge distribution of the β -lactam C7–O8 carbonyl group could be different in free *versus* enzyme-bound Pen G. The last two points were addressed by changing the charge distribution of the C7–O8 atoms and of the main-chain NH bonds of Ser70 and Ala237 in a way that

transfers the O8 partial charge onto the main-chain nitrogen atoms of residues 70 and 237, through the hydrogen bonds (2.7 Å and 3.0 Å) that comprise the oxyanion hole [8]. This appeared to be the simplest way to estimate the effect of the significant local dipoles generated by the Met69–Ser70 and Gly236–Ala237 peptide bonds which are nearly parallel to the oxyanion hydrogen bonds. In addition, this observation may explain why the (ϕ, ψ) dihedral angles of residue 69 are found outside the low-energy areas of the Ramachandran plot in all class A β -lactamase structures [9]. Transferring the O8 partial charge decreases the Ser70 pK_a by 10.9 pH units (Table 2), in line with the proposal that each of these hydrogen bonds contributes about 5 kcal mol⁻¹ [21], and does not significantly affect the pK_a of Lys73, located 3.0 Å away.

The kinetic data of mutant proteins in which Lys234 is substituted by threonine, alanine, glutamate or histidine [18–20] indicates that the enzyme activity is reduced by 100-fold. One can expect that these mutations affect the pK_a s of Lys73 and Ser70. The pK_a of Lys73 was calculated to be 13.0 in the Lys234→Thr TEM1 enzyme and increases to 20.4 upon Pen G binding (Table 2). This indicates that Lys73 is already protonated in the free mutant protein and this is confirmed by the identical enzyme activity measured for the Lys73→Arg β -lactamase I mutant enzyme [17,19].

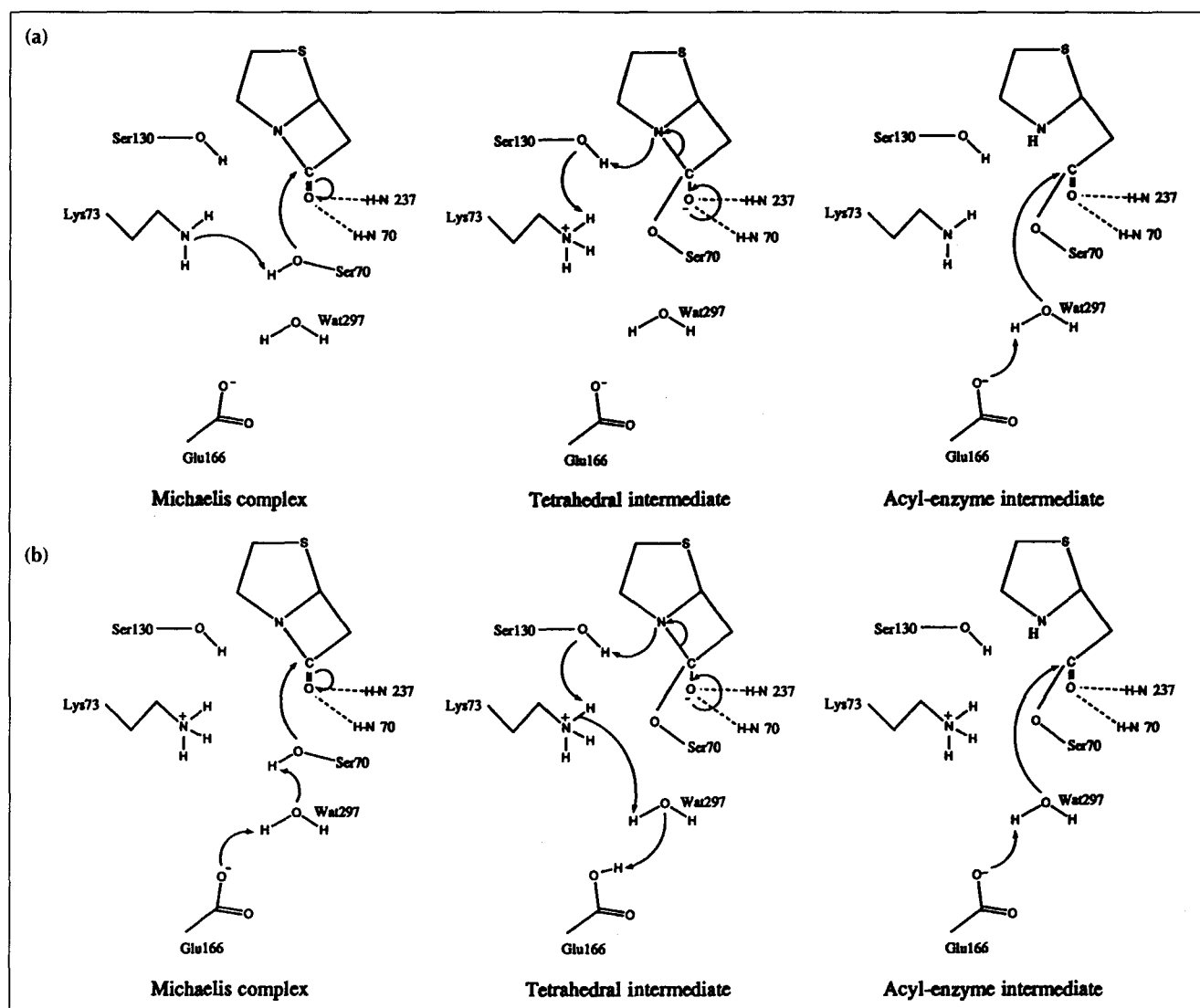


Fig. 5. Schematic representation of the two acylation reactions. (a) In the WT enzyme where Lys73 is unprotonated in the free enzyme [8]. (b) In the site-directed Lys73→Arg and Lys234→Thr mutant proteins where residue 73 is protonated in the free enzyme.

In the Lys234→Thr and Lys73→Arg mutant enzymes, Lys73 cannot be the proton acceptor of the Ser70 hydroxyl group and another proton acceptor has to be identified. The active-site structure suggests that Glu166, through the buried water molecule Wat297 located between Glu166 and Ser70 (2.8 Å distant from each), can play this role. This water molecule could act as a proton relay and assist the nucleophilic attack on the β -lactam C7 carbonyl carbon atom by Ser70 O γ , through the concerted abstraction of the Ser70 hydroxyl group proton and protonation of Glu166 (Fig. 5b). In this case, the protonated Lys73 becomes involved in the formation of a tetrahedral intermediate, through a proton shuffle between Ser130, Lys73, Wat297, and Glu166, leading to the formation of an acyl-enzyme complex ready for deacylation. The proton acceptor Glu166/Wat297 was suggested by Lamotte-Brasseur *et al.* [23] who had assumed that Lys73 was protonated in the WT enzyme. This acylation mechanism appears less efficient than in the WT enzyme because, in addition to the loss of the 15 kJ that

may lower the energy barrier for Ser70 deprotonation, it involves a larger number of proton transfers that may also contribute to the 100-fold reduction of the acylation rate constant, k_2 , measured for the Lys234→Thr and Lys73→Arg mutant enzymes [17]. The respective locations and distances between the carboxylate side chain of Glu166, the water, and the Ser70 O γ partners are also of importance in this process and k_2 should, therefore, be reduced upon a Glu166→Asp mutation. It was indeed found that the double mutant Lys73→Arg/Glu166→Asp displays an additional 100-fold decrease in k_2 compared with that of the single mutant Lys73→Arg [17].

The relatively low pK_a of 10.7 for Ser70 in the free Lys234→Thr TEM1 mutant enzyme (Table 2) may indicate that Ser70 is more reactive than in the WT enzyme. Binding of Pen G increases the pK_a of Ser70 by 21.2 pH units in this mutant and therefore deactivates Ser70 O γ , whereas a substrate devoid of the carboxylate group on the thiazolidine ring, such as penicillanyl alcohol, only

increases the pK_a of Ser70 by 5.7 pH units (Table 2). This substrate should therefore more readily form an acyl-enzyme with such mutant proteins and indeed, it displays a k_{cat} value eightfold higher than that of phenoxymethylpenicillin [18]. These kinetic data show that the substrate carboxylate effect on the Ser70 pK_a is poorly estimated, as already suspected: in the above case, it amounts to 15.5 pH units (21.2–5.7) and, if true, would lead to a larger difference in the k_{cat} values between penicillanyl alcohol and phenoxymethylpenicillin. The mechanism depicted in Figure 5b emphasizes the importance of the Glu166 and Lys73 protonation states. This is also indicated by the bell-shaped k_{cat}/K_M versus pH profile for the Lys234→Ala protein with penicillanyl alcohol as a substrate, which shows two ionizations, at $pK_1=5$ and $pK_2=11$ [18], in agreement with the expected pK_a of Glu166 and the calculated pK_a of Lys73 ($pK_a=13.0$).

The natural mutants of TEM1, identified from bacteria that are resistant to antibiotic treatment, have accordingly extended substrate specificities, but no mutation occurs at position 234, and none of the others which occur should affect the protonation state of Lys73. A charged residue at position 73 (i.e. Lys73→Arg or Lys234→X, where X is not arginine), is not known to occur spontaneously but was produced by site-directed mutagenesis. For these mutant enzymes we suggest an alternative mechanism for acylation (Fig. 5b). The idea of alternative mechanisms for a given enzyme may seem unlikely, but a coenzyme analogue of liver alcohol dehydrogenase, designed from the enzyme X-ray structure to interfere with the alcohol substrate-binding site, has been shown to induce a different mechanism [24]. The 'ordered bi-bi mechanism', expressing the sequential binding of NAD^+ and the conformational change of the protein prior to substrate binding, became a 'rapid equilibrium random bi-bi mechanism' in the presence of this coenzyme analogue.

The deacylation step

Deacylation is promoted by a proton transfer from the crystallographic water molecule, Wat297, to the carboxylate group of Glu166. This generates the nucleophilic hydroxyl group that attacks the ester carbonyl carbon of the acyl-enzyme intermediate. Electrostatic calculations on the acyl-enzyme complex show that the potential difference between Glu166 and the ester carbonyl carbon of the acyl-enzyme amounts to about 150 kTe^{-1} ($-125 kTe^{-1}$ at the carboxylate and $+25 kTe^{-1}$ at the ester carbonyl carbon) (Fig. 6). Hence, the water molecule, located at 2.8 Å from the Glu166 carboxylate in the direction of the ester carbonyl carbon, is experiencing a steep potential gradient amounting to 30 $kTe^{-1} \text{ Å}^{-1}$ that will aid in polarizing the water molecule and direct the proton and hydroxyl groups towards Glu166 and the ester carbonyl carbon, respectively. To evaluate the contribution of Glu166 to this gradient, we also computed the electrostatic potential in the acyl-enzyme complex with no atomic charges assigned to Glu166. The carboxylate group was now at a $-15 kTe^{-1}$ potential surface, which arises from the main-chain oxygen atoms of residues 104, 105, 130, 131, 165, and 167, and the side chains of residues 104, 106, 131, 136, 168, 170, and 240. This generates an 8 $kTe^{-1} \text{ Å}^{-1}$ gradient between Glu166 and the acyl-enzyme carbonyl carbon, similar to that computed for the Glu166→Asn TEM1 mutant protein (10 $kTe^{-1} \text{ Å}^{-1}$). This mutant protein, which was used to solve the acyl-enzyme structure and not reported to display any structural differences from the WT enzyme, lacks a defined proton acceptor. Nevertheless it deacylates, albeit slowly [11]. This might be due to the 10 $kTe^{-1} \text{ Å}^{-1}$ gradient, present in this protein. In β -lactamase I, k_3 is 1000 times lower upon a Glu166→Asp substitution [17]. In TEM1, the same mutation leads to accumulation of the acyl-enzyme and poor deacylation [11], and the calculated gradient is 20 $kTe^{-1} \text{ Å}^{-1}$. It thus seems that the active site structure provides a small intrinsic electrostatic potential gradient

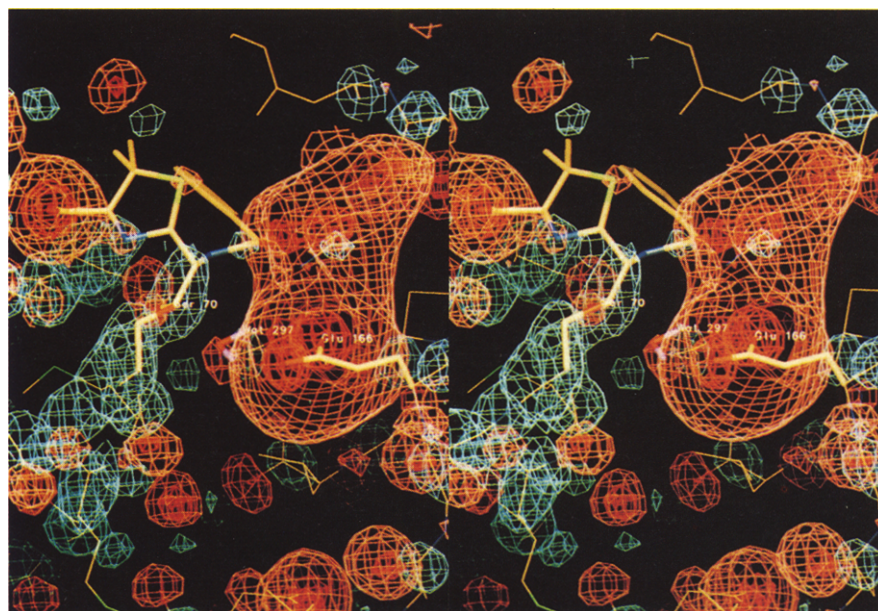


Fig. 6. Map of the electrostatic potential generated by the acyl-enzyme drawn at different contour levels varying from $-125 kTe^{-1}$ (red) at Glu166 to $+25 kTe^{-1}$ (blue) at the ester carbonyl carbon. The deacylating Wat297, in the centre of the picture, is located between Glu166 and the ester bond (Ser70) at a $-45 kTe^{-1}$ potential surface (orange).

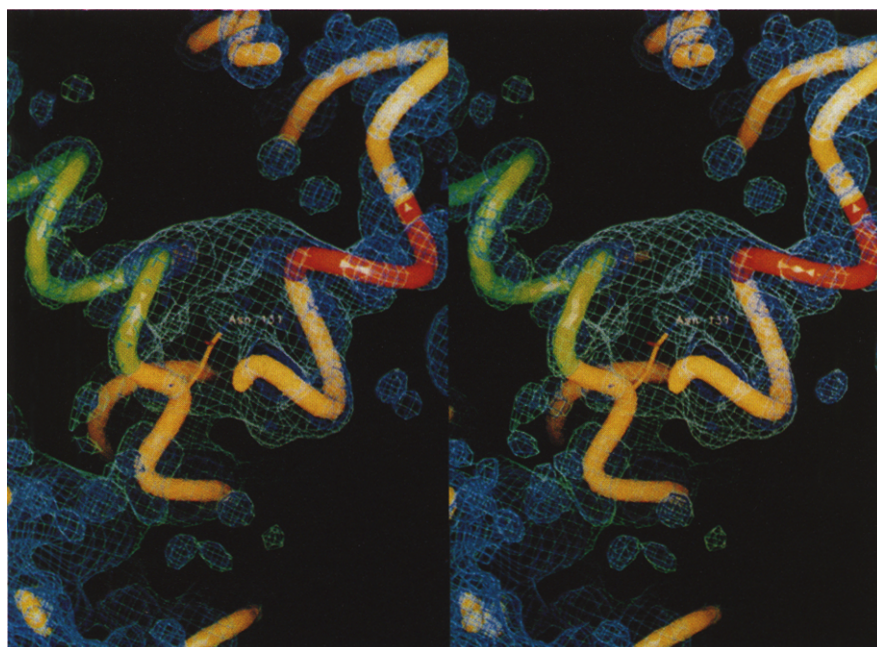


Fig. 7. Comparison of the $+20 \text{ kTe}^{-1}$ potential maps around residue 131 in the structure of the WT enzyme (dark blue) and in the modelled Asp131→Asn mutant (light blue). The backbone of the enzyme is shown in yellow, helix H3 in red, and helix H5 in green.

and that the proper positioning of an acidic group naturally increases its magnitude to an extent that might contribute to the high deacylation rate constant ($k_3=1500 \text{ s}^{-1}$).

The function of Asp131

The buried and invariant Asp131 is immersed in the -20 kTe^{-1} negative electrostatic potential as described above, and its carboxylate group is hydrogen bonded to the main-chain nitrogen atoms of residues 108, 109, 133, and 134. These residues are at the N termini of helices H3 (109–111) and H5 (132–142) [9]; the stabilization of those local dipoles could explain the invariance and the structural role of Asp131. This hypothesis is reminiscent of the sulphate-binding protein of *Salmonella typhimurium* where site-directed mutagenesis demonstrated the role of local dipoles from three helices in binding of the sulphate ion [25]. The electrostatic calculation performed after a modelled substitution of Asp131 by the most conservative residue, asparagine, showed the emergence of a very broad $+20 \text{ kTe}^{-1}$ positive potential that immersed the N termini of helices H3 and H5 (Fig. 7). Although we are aware that the microscopic situation in this region could be improperly described by the macroscopic continuum calculation [26], the inversion of potential to such a large extent in the Asp131→Asn protein compared with the WT enzyme indicates that strong favourable charge–helix interactions may be involved in the WT enzyme. Such interactions have been demonstrated in thermostable T4 lysozyme mutants [27] and in model peptides [28], and are consistent with the very poor expression of the Asp131→Gly mutant protein [29]. In addition, since the calculations showed that the potential gradient between Glu166 and the ester carbonyl carbon of the acyl–enzyme is not sensitive to the substitution, we may conclude that the major function of Asp131 is to stabilize protein folding.

Biological implications

With a $k_{\text{cat}}/K_{\text{M}}$ value of about $10^7 \text{ M}^{-1} \text{ s}^{-1}$, catalysis by class A β -lactamases is nearly a diffusion-controlled reaction. There has been evolutionary pressure on β -lactamases to broaden their substrate specificities but neither engineered mutants nor those isolated so far from natural sources have shown improved catalytic efficiency on the benzylpenicillin (Pen G) substrate. Hence, it seems that optimal conditions are met within the original *Escherichia coli* TEM1 enzyme, a penicillinase belonging to the class A β -lactamases. The physico-chemical and electrostatic features shown in this work support this contention.

Several mechanisms for the class A β -lactamases have been postulated. Kinetic characterization of site-directed mutants and X-ray structure determinations of the TEM1 enzyme were important steps towards the rational understanding of the structure–function relationships. Although amino acids essential for catalysis have been identified (Ser70, Lys73, Glu166, and Lys234), their exact mode of action (except for the acylating Ser70) and interrelations have been a matter of debate. The electrostatic potential distributions and pK_{a} shifts, both in the free enzyme and in the Michaelis and acyl–enzyme complexes of the wild-type enzyme, suggest an essential role for the unprotonated and solvent-shielded Lys73. We propose that substrate binding triggers the acylation reaction because it raises the pK_{a} of the active site Lys73 (by 6.4 pH units for Pen G). Its protonation in the Michaelis complex then provides 15 kT (9 kcal mol^{-1}) that may contribute by lowering the energy barrier for Ser70 deprotonation and thereby favour the nucleophilic attack on the substrate. Hydrolysis of

the acyl-enzyme complex is promoted by a proton transfer from the crystallographic water molecule, Wat297, to Glu166. This generates the nucleophilic hydroxyl group that attacks the ester carbonyl carbon of the acyl-enzyme. A steep electrostatic potential gradient, amounting to about $30 \text{ kTe}^{-1} \text{ \AA}^{-1}$, aids in polarizing the water molecule and directs the proton and hydroxyl groups. In enzymes where the gradient is of smaller magnitude, the deacylation step is considerably slower than in the wild-type enzyme.

In mutant proteins where protonation of residue 73 is imposed, the acylation pathway described for the wild-type enzyme cannot operate. Instead, an alternative and catalytically less efficient pathway, involving the Glu166/Wat297 couple acting as proton acceptor, can be used in these enzymes. This situation, which has been revealed by site-directed mutagenesis, may not be specific to the Class A β -lactamases and it might be interesting to consider the possibility of alternative mechanisms in other cases.

Materials and methods

Enzyme coordinates

The atomic coordinates of TEM1 were taken from the 1.8 \AA resolution refined X-ray structure [9] (Brookhaven Data Bank entry: 1BTL). The structure includes 199 water molecules and one sulphate ion provided by the crystallization conditions. This ion has no biological significance and was discarded from the calculations as well as 33 water molecules that do not exchange hydrogen bonds with protein atoms. All other water molecules were considered as part of the protein and have an average temperature factor of 14.6 \AA^2 . The different mutants were modelled on the structure of the WT enzyme with the program O [30]. Polar hydrogen positions were built and energy-minimized using the program X-PLOR [31]; new sets were generated for each mutant and each protonation state. None of the mutations introduced steric constraints into the protein structure. Solvent accessibilities [32] were computed with the program SURFACE from the CCP4 suite [33].

Modelling of complexes

The acyl-enzyme model was constructed according to the description given by Strynadka *et al.* [8]. The Michaelis complex was derived from the acyl-enzyme complex by closing the β -lactam ring by rotation of the N4-C5-C6-C7 torsion angle to its known value (5.4°) [34]. Structural constraints and interactions between protein and substrate are such that this rotation could only alter the position of the thiazolidine ring so as to maintain the positions of the β -lactam ring carbonyl and of the NHCO group at C6. In these models, five crystallographic waters (Wat323, Wat391, Wat404, Wat422, and Wat472) that occupy the substrate-binding site in the free enzyme were removed. Coordinates and charges of free Pen G were obtained by energy minimization in PCMODEL (Serena Software, Bloomington, IN). For the acyl-enzyme complex, the charges were obtained by energy minimization of penicilloic ethyl ester.

Numerical treatment

For evaluation of potential fields, we used the DelPhi package [35,36] which solves the linearized Poisson-Boltzmann

equation by a finite difference method. The TEM1 structure has a length of about 57 \AA which, together with the original DelPhi grid ($65 \times 65 \times 65$ grid points), gives a resolution of about one grid point per \AA . This was considered insufficient and the grid was extended to $129 \times 129 \times 129$ points. Two dummy atoms were introduced to control the position of the molecule within the grid. At a 'perfil' of 100%, these dummy atoms are located at opposite ends of the diagonal of the cubic grid in such a way that the longest dimension of the protein molecule, including its solvent-accessible surface (computed with a probe radius of 1.4 \AA), falls exactly within the grid. The atoms were assigned Connolly radii provided with the DelPhi package. A 2.0 \AA thick ion exclusion layer was added and the ionic strength of the bulk was set to 145 mM . The protein moiety was assigned a relative dielectric constant of 3.0 while that of the bulk was set to 80. Atomic charges were taken from the 'toph19.pro' file in X-PLOR [31,37] and distributed over the grid points according to an algorithm described by Gilson *et al.* [38]. This algorithm gives more accurate potentials at close distances than a traditional distribution over eight closest grid points. Charges of neutral lysines and anionic serines were obtained with PCMODEL. Analysis of the structure implied that all residues, except those stated in this work, could be kept in their normal protonation state at pH 7.8. Independence from chosen grid origin was verified by repeating the calculations with the geometric centre of protein plus dummy atoms placed at seven different grid points (the grid centre itself and its six closest neighbours). A three-step focusing protocol (15%, 60%, and 100% 'perfiles') was used with the Debye-Hückel potential of the equivalent dipole to the molecular charge distribution as boundary condition in the initial step [36]. The grid size was 0.52 \AA (1.92 grid points per \AA) in the last step.

Calculation of pK_a s

Three types of electrostatic energy contributions must be considered to evaluate the difference in the titration behaviour of an ionizable group in a protein and the same group in a model compound such as a free amino acid in bulk water [39,40]: first, the interaction of the group with the polarization that its charges induce in the protein and in the model (Born solvation energy, $\Delta\Delta G_{\text{Born}}$); second, the interaction of the group with partial charges, such as the peptide dipoles (back-ground charge interactions, $\Delta\Delta G_{\text{back}}$); third, the interaction of the group with other titrating groups in the protein. A rigorous treatment of titration should consider that the protonation state of a group depends on the protonation states of other titrating groups, which themselves are also pH dependent. Therefore, those interaction energies should be evaluated and a Boltzmann sum made over all possible energy states, which will be 2^N , where N equals the number of titratable sites in the protein. The process has been thoroughly outlined [40,41]. This statistical mechanical approach still has to cope with the inaccuracy of the protein dielectric, treated as a constant although it is a function of coordinates. The simplification we have made was based on a careful analysis of the TEM1 structure whereupon the protonation states of the other titrating sites were simply included in the background charge interaction energies when evaluating the pK_a of a certain residue. That is:

$$pK_a = pK_a^{\text{model}} - (kT \ln 10)^{-1} (\Delta\Delta G_{\text{Born}} + \Delta\Delta G_{\text{back}})$$

where pK_a^{model} is the side chain pK_a of a free amino acid [42] (the side chain of a free serine was assumed to have $pK_a = 16$, like ethanol). This simplification, rigorously valid when the investigated group is the only one that titrates in the analyzed pH range, was confirmed by the consistency with experimental

data. The model compounds were constructed by isolating the actual side chain, together with its backbone (the used charge set gives a neutral charge distribution of all backbones except termini), from the structure.

The calculation made to evaluate how the pK_a of Ser70 may be affected by the charge distribution of the β -lactam C7–O8 carbonyl group and of the NH bonds of residues 70 and 237 was carried out as follows. To get an estimate of the effect of the oxyanion hole in cancelling out the O8 partial charge, this was transferred in equal parts to the main-chain nitrogen atoms of residues 70 and 237. No additional polarization of the substrate carbonyl group compared with that of unbound Pen G was assumed. The charge distribution was, in free enzyme and Pen G: C7 +0.3; O8 –0.5; N70 –0.35; H70 +0.25; N237 –0.35; H237 +0.25; and after charge transfer: C7 +0.3; O8 0.0; N70 –0.60; H70 +0.25; N237 –0.60; H237 +0.25.

Hardware

The program O was run on an Evans and Sutherland ESV/30-33 and PCMODEL on an IBM RS/6000 workstation. All other software packages were run on a Digital DEC 3000/400 Alpha workstation (96 Mb RAM). A pK_a calculation required about one hour of CPU time.

Acknowledgements: We thank Dr Emmanuel Courcelle for his excellent assistance on informatics and Dr Martin Welch for correcting the English of the manuscript. We are also grateful to Prof Jean Devillers for general discussions on energy minimization. This work was financed, in part, by the Institut National de la Santé et de la Recherche Médicale (contract no. 930612) and by ARC (contract no. 6564). The Service Scientifique de l'Ambassade de France à Stockholm is gratefully acknowledged for financial support to PS.

References

- Ambler, R.P., et al., & Waley, S.G. (1991). A standard numbering scheme for the class A β -lactamases. *Biochem. J.* **276**, 269–272.
- Bush, K. (1989). Characterization of β -lactamases. *Antimicrob. Agents Chemother.* **33**, 259–263.
- Christensen, H., Martin, M.T. & Waley, S.G. (1990). β -lactamases as fully efficient enzymes. *Biochem. J.* **266**, 853–861.
- Dideberg, O., et al., & Ghuyssen, J.-M. (1987). The crystal structure of the β -lactamase of *Streptomyces albus* G at 0.3 nm resolution. *Biochem. J.* **245**, 911–913.
- Herzberg, O. (1991). Refined crystal structure of β -lactamase from *Staphylococcus aureus* PC1 at 2.0 Å resolution. *J. Mol. Biol.* **217**, 701–719.
- Knox, J.R. & Moews, P.C. (1991). β -lactamase of *Bacillus licheniformis* 749/C. Refinement at 2 Å resolution and analysis of hydration. *J. Mol. Biol.* **220**, 435–455.
- Jelsch, C., Lenfant, F., Masson, J.-M. & Samama, J.-P. (1992). β -lactamase TEM1 of *E. coli*. Crystal structure determination at 2.5 Å resolution. *FEBS Lett.* **299**, 135–142.
- Strynadka, N.C.J., et al., & James, M.N.G. (1992). Molecular structure of the acyl-enzyme intermediate in β -lactam hydrolysis at 1.7 Å resolution. *Nature* **359**, 700–705.
- Jelsch, C., Mourey, L., Masson, J.-M. & Samama, J.-P. (1993). Crystal structure of *Escherichia coli* TEM1 β -lactamase at 1.8 Å resolution. *Proteins* **16**, 364–383.
- Herzberg, O. & Moul, J. (1991). Penicillin-binding and degrading enzymes. *Curr. Opin. Struct. Biol.* **1**, 946–953.
- Adachi, H., Ohta, T., Matsuzawa, H. (1991). Site-directed mutants, at position 166, of RTE-1 β -lactamase that form a stable acyl-enzyme intermediate with penicillin. *J. Biol. Chem.* **266**, 3186–3191.
- Oefner, C., et al., & Winkler, F.K. (1990). Refined crystal structure of β -lactamase from *Citrobacter freundii* indicates a mechanism for β -lactam hydrolysis. *Nature* **343**, 284–288.
- Dao-pin, S., Anderson, D.E., Baase, W.A., Dahlquist, F.W. & Matthews, B.W. (1991). Structural and thermodynamic consequences of burying a charged residue within the hydrophobic core of T4 lysozyme. *Biochemistry* **30**, 11521–11529.
- Hedges, R.W., Datta, N., Kontomichalou, P. & Smith, J.Y. (1974). Molecular specificities of R factor determined beta-lactamases: correlation with plasmid compatibility. *J. Bacteriol.* **117**, 56–62.
- Delaire, M., Labia, R., Samama, J.-P. & Masson, J.-M. (1992). Site-directed mutagenesis at the active site of *E. coli* TEM1 β -lactamase. *J. Biol. Chem.* **267**, 20600–20606.
- Zafaralla, G., Manavathu, E.K., Lerner, S.A. & Mobashery, S. (1992). Elucidation of the role of arginine-244 in the turnover processes of class A β -lactamases. *Biochemistry* **31**, 3847–3852.
- Gibson, R.M., Christensen, H. & Waley, S.G. (1990). Site-directed mutagenesis of β -lactamase I. Single and double mutants of Glu 166 and Lys 73. *Biochem. J.* **272**, 613–619.
- Ellerby, L.M., Escobar W.A., Fink, A.L., Mitchinson, C. & Wells, J.A. (1990). The role of lysine 234 in β -lactamase catalysis probed by site-directed mutagenesis. *Biochemistry* **29**, 5797–5806.
- Lenfant, F., Labia, R. & Masson, J.-M. (1991). Replacement of lysine 234 affects transition state stabilization in the active site of β -lactamase TEM1. *J. Biol. Chem.* **266**, 17186–17194.
- Brannigan, J., et al., & Frère, J.-M. (1991). The mutation Lys234/His yields a class A β -lactamase with a novel pH-dependence. *Biochem. J.* **278**, 673–678.
- Warshel, A., Naray-Szabo, G., Sussmann, F. & Hwang, J.-K. (1989). How do serine proteases really work? *Biochemistry* **28**, 3629–3637.
- Daggett, V., Schröder, S. & Kollman, P. (1991). Catalytic pathway of serine proteases: classical and quantum mechanical calculations. *J. Am. Chem. Soc.* **113**, 8926–8935.
- Lamotte-Brasseur, J., Dive, G., Dideberg, O., Charlier, P., Frère, J.-M. & Ghuyssen, J.-M. (1991). Mechanism of acyl transfer by the class A serine β -lactamase of *Streptomyces albus* G. *Biochem. J.* **279**, 213–221.
- Samama, J.-P., Hirsch, D., Goulas, P. & Biellmann, J.-F. (1986). Dependence of the substrate specificity and kinetic mechanism of horse-liver alcohol dehydrogenase on the size of the C-3 pyridinium substituent; 3-benzoylpyridine-adenine dinucleotide. *Eur. J. Biochem.* **159**, 375–380.
- He, J.J. & Quirocho, F.A. (1993). Dominant role of local dipoles in stabilizing uncompensated charges on a sulfate sequestered in a periplasmic active transport protein. *Protein Sci.* **2**, 1643–1647.
- Åqvist, J., Luecke, H., Quirocho, F.A. & Warshel, A. (1991). Dipoles localized at helix termini of proteins stabilize charges. *Proc. Natl. Acad. Sci. USA* **88**, 2026–2030.
- Nicholson, H., Anderson, D.E., Dao-pin, S. & Matthews, B.W. (1991). Analysis of the interaction between charged side-chains and the α -helix dipole using designed thermostable mutants of phage T4 lysozyme. *Biochemistry* **30**, 9816–9819.
- Huyghues-Despointes, B.M.P., Scholtz, J.M. & Baldwin, L. (1993). Effect of a single aspartate on helix stability at different positions in a neutral alanine-based peptide. *Protein Sci.* **2**, 1604–1611.
- Jacob, F., Joris, B., Lepage, S., Dusart, J. & Frère J.-M. (1990). Role of the conserved amino acids of the 'SDN' loop (Ser130, Asp131 and Asn132) in a class A β -lactamase studied by site-directed mutagenesis. *Biochem. J.* **271**, 399–406.
- Jones, T.A., Zou, J.-Y., Cowan, S.W. & Kjeldgaard, M. (1991). Improved methods for building protein models in electron density maps and the location of errors in these models. *Acta Crystallogr. A* **47**, 110–119.
- Brünger, A.T. (1992). *X-PLOR Version 3.1: A System for X-ray Crystallography and NMR*. Yale University, New Haven, CT.
- Lee, B. & Richards, F.M. (1971). The interpretation of protein structures: estimation of static accessibility. *J. Mol. Biol.* **55**, 379–400.
- Collaborative Computational Project, Number 4 (1994). The CCP4 suite: programs for protein crystallography. *Acta Crystallogr. D* **50**, 760–763.
- Dexter, D.D. & van der Veen, J.M. (1978). Conformations of penicillin G: crystal structure of procaine penicillin G monohydrate and a refinement of the structure of potassium penicillin G. *J. Chem. Soc. (Perkin Trans. I)*, 185–190.
- Nicholls, A. & Honig, B. (1991). A rapid finite difference algorithm, utilizing successive over-relaxation to solve the Poisson–Boltzmann equation. *J. Comput. Chem.* **12**, 435–445.
- Sharp, K.A. & Nicholls, A. (1989). *DelPhi (v. 3.0) Manual*. Dept. of Biochemistry and Molecular Biophysics, Columbia University, NY.
- Brooks, B.R., Brucoleri, R.E., Olafson, B.D., States, D.J., Swaminathan, S. & Karplus, M. (1983). CHARMM: a program for macromolecular energy, minimization and dynamics calculations. *J. Comput. Chem.* **4**, 187–217.
- Gilson, M.K., Sharp, K.A. & Honig, B.H. (1987). Calculating the electrostatic potential of molecules in solution: method and error assessment. *J. Comput. Chem.* **9**, 327–335.
- Tanford, C. & Kirkwood, J.G. (1957). Theory of protein titration curves. I. General equations for impenetrable spheres. *J. Am. Chem. Soc.* **79**, 5333–5339.

40. Bashford, D. & Karplus, M. (1990). pK_a 's of ionizable groups in proteins: atomic detail from a continuum electrostatic model. *Biochemistry* **29**, 10219–10225.
41. Yang, A.-S., Gunner, M.R., Sampogna, R., Sharp, K. & Honig, B. (1993). On the calculation of pK_a s in proteins. *Proteins* **15**, 252–265.
42. Dawson, R.M.C., Elliott, D.C., Elliott, W.H. & Jones, K.M. (1986). *Data for Biochemical Research*. (3rd edn), pp. 1–31, Clarendon Press, Oxford.
43. Lenfant, F. (1991). Etude du site actif de la β -lactamase TEM-1 d'*Escherichia coli* par mutagenèse dirigée. [PhD thesis]. INSA, Toulouse, France.
44. Kraulis, P.J. (1991). MOLSCRIPT: a program to produce both detailed and schematic plots of protein structures. *J. Appl. Crystallogr.* **24**, 946–950.

Received: 7 Nov 1994; revisions requested: 30 Nov 1994;
revisions received: 19 Apr 1995. Accepted: 2 May 1995.